

## Electronic structure of the Jahn-Teller-distorted group-V-impurity–vacancy pairs in silicon

Xi-Qing Fan, San-Guo Shen, and De-Xuan Zhang

*Department of Physics, Zhengzhou University, Zhengzhou 450052, Henan, People's Republic of China*

(Received 16 January 1990)

An attempt is made to combine tight-binding band-structure theory with the defect theory of Hjalmarson *et al.* [Phys. Rev. Lett. **44**, 810 (1980)] to calculate wave functions of the electron localized near the Jahn-Teller-distorted group-V-impurity–vacancy pair in Si. The effect of the defect potential is extended to the nearest-neighbor sites, including both diagonal and off-diagonal matrix elements of the defect potential. From the calculated wave function, the hyperfine interactions of an electron with Si or impurity (P,As,Sb) nuclei near the vacancy are obtained to compare with those determined experimentally by electron paramagnetic resonance and electron-nuclear double resonance. Good agreement is obtained for nearest-neighbor atoms of PV, AsV, and SbV, for which similarities are exhibited among these defects. We also predict the hyperfine interaction for BiV. The use of the defect-pair “molecule” model of Sankey and Dow [Phys. Rev. B **26**, 3243 (1982)] leads to an estimate of  $\sim 0.1$  eV for the magnitude of the Jahn-Teller distortion.

### I. INTRODUCTION

In the past, much experimental information has been gathered about vacancy-related defects in monocrystalline silicon,<sup>1</sup> among which are vacancy clusters, such as divacancies, trivacancies, tetravacancies, and even pentavacancies, as well as vacancies paired with impurity atoms. An important class of vacancy-related defects is the complex of vacancies with group-III, -IV, and -V substitutional impurities. The most important feature of the various substitutional-impurity–vacancy pairs has been identified with the use of electron paramagnetic resonance (EPR) or electron-nuclear double-resonance (ENDOR) techniques. Striking differences exist between these centers. In fact, the similarities in features are exhibited only among the phosphorus-, arsenic-, and antimony-, or bismuth-vacancy pairs. The energy levels, in analogy with  $E_c - 0.4$  eV, have been determined for these defects,<sup>2,3</sup> and their EPR and ENDOR spectra also show a high degree of formal similarity to one another.<sup>4,5</sup> The pair “molecule” model by Sankey and Dow<sup>6</sup> has given a qualitative account of these common features. The impurity-vacancy pair cannot alter the deep vacancy level very much, because it is derived from the  $T_2$  level; however, none of the papers published, to our knowledge, presents calculations of the hyperfine interactions of distorted group-V-impurity–vacancy pair in silicon which may allow direct comparison with EPR or ENDOR experimental results. The hyperfine interaction for monovacancies,<sup>7</sup> divacancies,<sup>8</sup> trivacancies,<sup>9</sup> and tetravacancies<sup>10</sup> has been calculated by us in the central-cell-potential approximation or in the extended-potential approximation, and the results are in good agreement with experiment. The present paper represents a natural extension of our previous work to include that of the group-V-impurity–vacancy pairs.

In following the established custom<sup>11</sup> for theories of deep defect levels, the long-range Coulomb potential is

neglected, and only the short-range potential is considered. The potential introduced by the vacancy is adopted in the orbital-removal approximation and the potential of the impurity atom is constructed by the rules of Hjalmarson *et al.*<sup>11</sup> In the site representation, we construct the symmetric basis function of the point group belonging to these defects, and the zeroth-order symmetric wave function of the defect under the Jahn-Teller distortion is obtained with use of a tight-binding Green's-function method. The hyperfine interaction constants and g tensor shift are calculated. These calculated results are all found to be comparable to experiment. This means that the method mentioned above is successful in describing the similarity of the spectra for group-V-impurity–vacancy pairs in silicon.

### II. ATOMIC STRUCTURE OF THE DEFECT AND SYMMETRIC BASIS FUNCTION

From the EPR and ENDOR spectra of the group-V impurities, the atomic structure of the defects has been given by Watkins and Corbett<sup>4</sup> and Elkin and Watkins,<sup>5</sup> as shown in Fig. 1. The choice of the  $x, y, z$  coordinate system is along the crystal principal axes. The vacancy atom is at the origin (0,0,0). The impurity atom is at the lattice point (1, -1, 1) next to the vacancy, and the remaining three nearest-neighbor atoms are at the lattice points (-1, 1, 1) (1, 1, -1), and (-1, -1, -1).

For ease of representation, following Watkins and Corbett, we first visualize the construction of the defect qualitatively.<sup>4</sup> Initially an isolated lattice vacancy has four broken bonds associated with the four neighboring silicon atoms, the system has the symmetry of the  $T_d$  point group, and gives four degenerate one-electron orbitals. With replacement of an atom next to a vacancy by a group-V-impurity atom, the system is lowered to  $C_{3v}$  symmetry and an extra positive charge is added at this site. The defect is in the neutral charge state, and five

electrons are accommodated in these orbitals. Two electrons are paired in the  $c$  orbital; three of the remaining are in the set of  $a, b, d$  orbitals. Because of the degeneracy associated with the partially filled  $a, b, d$  orbitals, a spontaneous distortion takes place to remove this degeneracy. Viewed this way, the bent bond of silicon atoms 2 and 3, in Fig. 1(b), is formed, while an unpaired electron is most-

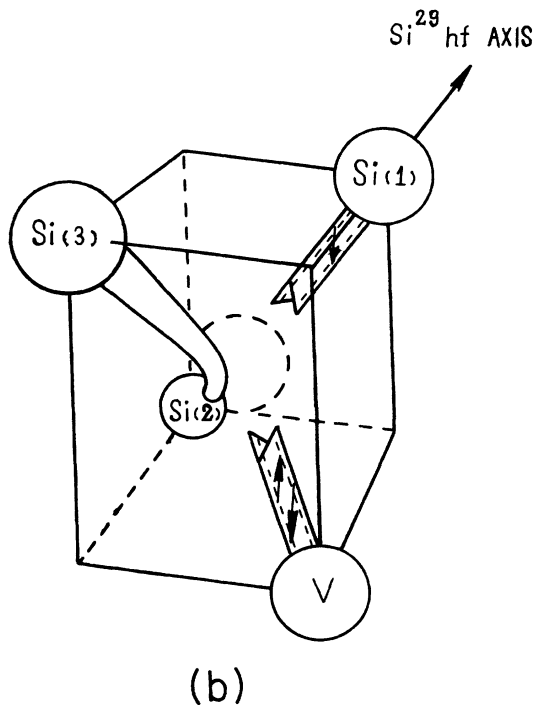
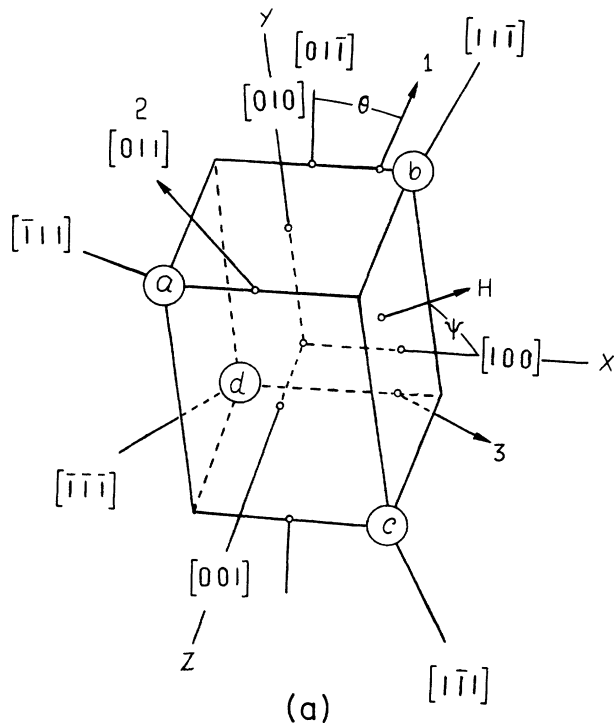


FIG. 1. The atomic structure of the defect: (a) the coordinate system and the atomic position, and (b) the model of the defect.

ly distributed in the orbital of the remaining silicon, and is presumably distributed over more distant silicon atoms surrounding the vacancy, and so the one-electron approximation can be used to describe the unpaired electron of the defect.

Upon imposition of the Jahn-Teller effect, the symmetry of the system is further lowered to  $C_{1h}$ , and the symmetric plane is the plane (001). Thus the atoms may be divided into two classes, the atoms on the symmetric plane are considered to belong to the mirror class, denoted  $M$ , and the atoms not on the symmetric plane belong to the general class, denoted  $G$ . Under the operators of  $C_{1h}$ , the atom positions belonging to the  $M$  class can only exchange with themselves, the atom positions of the  $G$  class may be exchanged between two atoms.

Let  $V_0$  represent the short-range potential introduced by the defect before the distortion (i.e., in the ideal case), the  $V_0$  has  $C_{3v}$  symmetry. After the distortion, the additional small potential  $\Delta V$  introduced has the lower symmetry  $C_{1h}$ . So the defect potential  $V$  may be decomposed into two parts:<sup>12</sup>

$$V = V_0 + \Delta V. \quad (1)$$

Hence the one-electron Hamiltonian,  $H = H_0 + V$  ( $H_0$  is the host one), has the point-group symmetry  $C_{1h}$ . Thus the wave function of the defect electron is comprised of the states that transform according to a definite irreducible representation of the point group  $C_{1h}$ . From the perturbation theory, the zeroth-order wave function of the nondegenerate state after the distortion can be constructed with use of the unperturbation wave function according to the symmetry  $C_{1h}$ . In the present article, we will calculate the symmetric wave function in the zeroth order.

Now we first construct the basis function for the irreducible representation of  $C_{1h}$ . By taking the center point in  $(1, -1, 1)a_0/8$ ,  $a_0$  being the lattice constant, all the atoms are in the shells labeled by an index  $R$ . Making use of the  $sp^3$  hybrid orbitals associated with the atoms in each shell, the symmetric basis function could be obtained in the following way.

The hybrid orbital directions of the atoms in silicon have two varieties, one is  $[\bar{1}11]$ ,  $[1\bar{1}\bar{1}]$ ,  $[1\bar{1}1]$ ,  $[\bar{1}1\bar{1}]$ , such as the vacancy atom in Fig. 1; the other is  $[111]$ ,  $[111]$ ,  $[\bar{1}\bar{1}\bar{1}]$ ,  $[111]$ , such as the four nearest-neighbor atoms. We denoted them in sequence by the numbers 1, 2, 3, 4. Then the hybrid orbital is labeled by a letter (for the atom) in Fig. 1, followed by a number. For instance, the symbol  $V_1$  represents the hybrid orbital pointing toward  $[\bar{1}11]$  for vacancy atom  $V$ ;  $B_4$  is the hybrid orbital for the atom  $b$  that points toward the  $[111]$  direction.

It is easy to obtain the basis function  $|IRm\rangle$  for a defined irreducible representation using the projection-operator technique; the  $|IRm\rangle$  are symmetry, orthogonal functions, and  $l$  denotes the irreducible representation  $A'$  or  $A''$  (both are one dimensional);  $R$  indexes the  $R$ th shell around the center points, and  $m$  marks the  $m$ th basis function of the  $R$ th shell transforming according to the irreducible representation  $l$ . Here we will only give part of the basis function of the  $A'$  representation. By

the above appointment, the vacancy and the impurity atoms form the shell  $R=0$ , each belonging to the  $M$  class; so their hybrid orbitals form the basis function, respectively.

For the vacancy atom,

$$\begin{aligned} |A'01\rangle &= (V_1 + V_4)/\sqrt{2}, \\ |A'02\rangle &= V_2, \\ |A'03\rangle &= V_3. \end{aligned} \quad (2)$$

For impurity atom,

$$\begin{aligned} |A'04\rangle &= (I_1 + I_4)/\sqrt{2}, \\ |A'05\rangle &= I_2, \\ |A'06\rangle &= I_3. \end{aligned} \quad (3)$$

In the shell  $R=1$ , the basis function for  $A'$  representation formed by the dangling bond of atoms  $a, d$  belonging to the  $G$  class is

$$|A'11\rangle = (A_1 + D_4)/\sqrt{2}, \quad (4)$$

which by the dangling bond of atom  $b$ , is

$$|A'12\rangle = B_2. \quad (5)$$

In this way, all of  $|lRm\rangle$  are represented by the atomic hybrid orbitals.

EPR and ENDOR experiments show that in each defect  $\sim 60\%$  of the total wave function is localized on the dangling bond of atom  $b$ . However, the  $B_2$  dangling bond only takes part in the symmetric combination for the irreducible representation  $A'$ , but does not appear in the symmetric combination for the irreducible representation  $A''$ . From these analyses, it is concluded that the defect lies only in an  $A'$  symmetry state.

### III. ELECTRONIC WAVE FUNCTION OF THE DEFECT

Adopting the Koster-Slater Green's-function method, the electron state  $|\psi\rangle$  bound by the short-range potential  $V$  satisfies the following equation:

$$|\psi\rangle = G(E)V|\psi\rangle. \quad (6)$$

With Green's function  $G(E) = 1/(E - H_0)$ ,  $H_0$  is the one-electron Hamiltonian for the host crystal, its eigenvalues  $E_{n\kappa}$  and the eigenvectors  $|n\kappa\rangle$  are given by the equation

$$H_0|n\kappa\rangle = E_{n\kappa}|n\kappa\rangle. \quad (7)$$

We now expand  $|\psi\rangle$  in terms of the basis function  $|A'Rm\rangle$ , i.e., in the lattice representation

$$|\psi\rangle = \sum_{Rm} |A'Rm\rangle \langle A'Rm|\psi\rangle \quad (8)$$

and decompose the defect potential as

$$V = \sum_{R,m} \sum_{R',m'} |A'Rm\rangle \langle A'Rm|V|A'R'm'\rangle \langle A'R'm'|. \quad (9)$$

As may be imagined, the electronic structure for the substitutional-impurity-vacancy pair is mainly determined by the vacancy and its neighbors, so that the defect potential  $V$  may be only expanded on the atoms next to the vacancy. Due to the Jahn-Teller distortion, the atoms  $a$  and  $d$  are near the vacancy; the atom  $b$  is away from the vacancy. In a rough approximation, the  $V$  is expanded on the atoms  $a, d$  for the shell  $R=1$ . The potential parameters that are introduced are then  $V_{mm} = \langle A'0m|V|A'0m\rangle$  ( $m=1,2,\dots,6$ ),  $V_{17} = \langle A'01|V|A'11\rangle = V_{71}$ , and  $V_{77} = \langle A'11|V|A'11\rangle$ . Substituting (8) and (9) in (6), we have

$$\begin{aligned} \langle A'Rm|\psi\rangle &= \sum_{n=1}^6 \langle A'Rm|G|A'0n\rangle C_n \\ &\quad + \langle A'Rm|G|A'11\rangle C_7, \end{aligned} \quad (10)$$

where the coefficients are

$$\begin{aligned} C_1 &= V_{11}\langle A'01|\psi\rangle + V_{17}\langle A'11|\psi\rangle, \quad C_2 = V_{22}\langle A'02|\psi\rangle, \\ C_3 &= V_{33}\langle A'03|\psi\rangle, \quad C_4 = V_{44}\langle A'04|\psi\rangle, \\ C_5 &= V_{55}\langle A'05|\psi\rangle, \quad C_6 = V_{66}\langle A'06|\psi\rangle, \\ C_7 &= V_{77}\langle A'11|\psi\rangle + V_{71}\langle A'01|\psi\rangle. \end{aligned} \quad (11)$$

For a lattice vacancy, in the orbital-removal approximation, there should be  $V_{11}, V_{22}, V_{33} \rightarrow \infty$ ,  $\langle A'01|\psi\rangle, \langle A'02|\psi\rangle, \langle A'03|\psi\rangle \rightarrow 0$ , so that  $C_1, C_2, C_3$  are the finite amount. From Eq. (10), we obtain three of the linear homogeneous equations of the  $c$  coefficients. After the unitary transformation, the basis function  $|A'04\rangle, |A'05\rangle, |A'06\rangle$  formed by the hybrid orbitals of the impurity atom may be represented in terms of its  $s$  and  $p$  orbital, and it is proved that

$$\begin{aligned} V_{44} &= \langle A'04|V|A'04\rangle = V_s, \\ V_{55} &= \langle A'05|V|A'05\rangle = V_p = V_{66}. \end{aligned} \quad (12)$$

Where  $V_s$  and  $V_p$  are the potential components of the  $s$  and  $p$  symmetry in the impurity atom, respectively. The value of  $V_s$  and  $V_p$  can be determined from the empirical approximate formula<sup>13</sup>

$$\begin{aligned} V_s &= \beta_s [\omega(s,i) - \omega(s,h)], \\ V_p &= \beta_p [\omega(p,i) - \omega(p,h)], \end{aligned} \quad (13)$$

where  $[\omega(s,i) - \omega(s,h)]$ ,  $[\omega(p,i) - \omega(p,h)]$  are the energy differences of the  $s, p$  orbital between the impurity atom and the host silicon atom; the parameters  $\beta_s = 0.8$  and  $\beta_p = 0.6$ . The values of  $V_s$  and  $V_p$  for relevant impurity atoms are listed in Table I. For the case of known  $V_s$  and  $V_p$ , the three linear homogeneous equations of the others may be obtained.

TABLE I. The potential due to the impurity atom.

Symmetric potential	P	As	Sb	Bi
$V_s$	-3.4068	-3.1282	-0.9134	-0.2569
$V_p$	-1.5438	-1.1810	-0.6131	-0.3735

In summary, the six linear homogeneous equations of  $c$  coefficients are

$$\begin{aligned}
& G_{11}C_1 + G_{12}C_2 + G_{13}C_3 + G_{14}C_4 \\
& \quad + G_{15}C_5 + G_{16}C_6 + G_{17}C_7 = 0, \\
& G_{21}C_1 + G_{22}C_2 + G_{23}C_3 + G_{24}C_4 \\
& \quad + G_{25}C_5 + G_{26}C_6 + G_{27}C_7 = 0, \\
& G_{31}C_1 + G_{32}C_2 + G_{33}C_3 + G_{34}C_4 \\
& \quad + G_{35}C_5 + G_{36}C_6 + G_{37}C_7 = 0, \\
& G_{41}C_1 + G_{42}C_2 + G_{43}C_3 + (G_{44} - 1/V_s) \\
& \quad C_4 + G_{45}C_5 + G_{46}C_6 + G_{47}C_7 = 0, \\
& G_{51}C_1 + G_{52}C_2 + G_{53}C_3 + G_{54}C_4 \\
& \quad + (G_{55} - 1/V_p)C_5 + G_{56}C_6 + G_{57}C_7 = 0, \\
& G_{61}C_1 + G_{62}C_2 + G_{63}C_3 + G_{64}C_4 + G_{65}C_5 \\
& \quad + (G_{66} - 1/V_p)C_6 + G_{67}C_7 = 0.
\end{aligned} \tag{14}$$

Here,  $G_{mn} = \langle A'0m | G | A'0n \rangle$ ,  $G_{m7} = \langle A'0m | G | A'11 \rangle$  ( $m, n = 1, 2, \dots, 6$ ). From the normalization condition  $\langle \psi | \psi \rangle - \langle \psi | VG^2V | \psi \rangle = 1$ , another equation of  $c$  coefficients is given by

$$-\sum_{m=1}^7 \sum_{n=1}^7 C_m \frac{dG_{mn}}{dE} C_n = 1. \tag{15}$$

The matrix element of the Green's function in Eqs. (14) and (15) can be calculated by

$$\begin{aligned}
\langle A'Rm | G | A'0m' \rangle &= \sum_{n,\kappa} \frac{\langle A'Rm | n\kappa \rangle \langle n\kappa | A'0m' \rangle}{E - E_{n\kappa}}, \\
\langle A'Rm | G | A'11 \rangle &= \sum_{n,\kappa} \frac{\langle A'Rm | n\kappa \rangle \langle n\kappa | A'11 \rangle}{E - E_{n\kappa}}.
\end{aligned} \tag{16}$$

In calculating Eq. (16), an empirical tight-binding Hamiltonian<sup>14</sup>  $H_0$  is used to describe the band structure of the host crystal, the summation on wave vector  $\kappa$  in the Brillouin zone is performed with use of the special  $\kappa$ -point method of Chadi and Cohen.<sup>15</sup> The values of the  $V_s, V_p$  and the matrix elements of the Green's function are substituted in Eq. (14); all the  $c$  coefficients can be solved from Eqs. (14) and (15), but they are the function of the defect energy  $E$ .

The above-calculated wave function of the unpaired electron localized near the defect will be used to obtain hyperfine interaction constants and to evaluate the  $g$ -tensor shift in Sec. IV.

#### IV. HYPERFINE INTERACTION AND THE $g$ TENSOR

In order to use the symmetric wave function  $\langle A'Rm | \psi \rangle$  to calculate the hyperfine interaction constants, we now expand the electronic state  $|\psi\rangle$  in terms of the atomic orbitals at the lattice site around the defect

$$|\psi\rangle = \sum_j (C_{js} |js\rangle + C_{jx} |jx\rangle + C_{jy} |jy\rangle + C_{jz} |jz\rangle), \tag{17}$$

where  $|js\rangle, |jx\rangle, |jy\rangle$ , and  $|jz\rangle$  are the  $ns$  and  $np$  atomic orbitals of the host or substitutional-impurity at the  $j$ th set;  $C_{js} = \langle js | \psi \rangle$ ,  $C_{jx} = \langle jp_x | \psi \rangle$ ,  $C_{jy} = \langle jp_y | \psi \rangle$ , and  $C_{jz} = \langle jp_z | \psi \rangle$  are obtained using the calculated  $\langle A'Rm | \psi \rangle$  for each shell.

As usual, the probability of the unpaired electron on the  $j$ th atom is represented by

$$\eta_j^2 = C_{js}^2 + C_{jx}^2 + C_{jy}^2 + C_{jz}^2, \tag{18}$$

and the percentage  $s$  and  $p$  character of the wave function by

$$\begin{aligned}
\alpha_j^2 &= C_{js}^2 / \eta_j^2, \\
\beta_j^2 &= (C_{jx}^2 + C_{jy}^2 + C_{jz}^2) / \eta_j^2, \\
\alpha_j^2 + \beta_j^2 &= 1.
\end{aligned} \tag{19}$$

It has been found in EPR and ENDOR<sup>4,5</sup> experiments that the hyperfine tensor for the substitutional-impurity-vacancy pair in silicon is nearly an axial symmetric one along the  $p$  orbital axis. In this approximation, principal values can then be parametrized  $(A_{\parallel})_j = a_j + 2b_j$ ,  $(A_{\perp})_j = a_j - b_j$ . The relationships between the constants  $a_j, b_j$  and  $\alpha_j^2, \beta_j^2, \eta_j^2$  are

$$\begin{aligned}
a_j &= (16\pi/3)(\mu_j/I_j)\mu_B a_j^2 \eta_j^2 |\psi_{ns}(0)|_j^2, \\
b_j &= \frac{4}{5}(\mu_j/I_j)\mu_B \beta_j^2 \eta_j^2 \langle r_{np}^{-3} \rangle_j,
\end{aligned} \tag{20}$$

where the isotropic part  $a_j$  is the Fermi constant interaction that is proportional to the probability density  $|\psi_{ns}(0)|_j^2$  of the unpaired electron at the site of the magnetic nucleus. The anisotropic part of the hyperfine interaction  $b_j$  is proportional to the expectation value  $\langle r_{np}^{-3} \rangle_j$  over the relevant atomic  $p$  orbital. In our calculation, the values of  $|\psi_{ns}(0)|_j^2, \langle r_{np}^{-3} \rangle_j$  are taken to be the same as those used in Refs. 4 and 5.

The hyperfine tensor calculated from Eq. (20) is purely axial symmetric and its axial direction is determined by the direction cosine which is proportional to  $C_{jx}, C_{jy}$ , and  $C_{jz}$ , respectively. The distorted substitutional-impurity-vacancy pair in silicon has a (011) mirror plane in which two of the  $|C_{jx}|, |C_{jy}|$ , and  $|C_{jz}|$  for the atoms located in the plane would be equal to each other, such as  $|C_{jx}| \neq |C_{jy}| = |C_{jz}|$ ; thus the axial direction of the hyperfine tensor arising from the atom for the  $M$  class is presented by the angle  $\theta$  between the axial direction and the  $\langle 011 \rangle$  direction,

$$\theta = \tan^{-1} \left[ \frac{C_{jx}}{|\sqrt{2}C_{jy}|} \right]. \tag{21}$$

We also want to calculate the  $g$  tensor pertinent to the dangling bond from the calculated wave function, but here the semiempirical theory is used. Because the full theoretical analysis of the  $g$  tensor should include the wave function  $|\psi_n\rangle$  and the energy levels  $E_n$  of excited states in the calculation, this is a cumbersome problem. In the following, we present the formula by Watkins and

Corbett,<sup>4</sup> and Phillips,<sup>16</sup> for calculating the  $g$  tensor to be used.

Generally, for the  $g$  tensor of the vacancy-type defect<sup>1</sup> with a dangling bond the axial symmetry approximation is adopted. Therefore a  $g$  tensor can be expressed by two principal values,  $g_{\parallel}$  and  $g_{\perp}$ , with the  $g_{\parallel}$  corresponding to the value along the axial direction. For many of vacancy-type defects, their  $g$  tensors are not always exactly axially symmetric. Thus the value  $g_{\perp}$  is chosen as the average of the two principal values which are closest; the third one is then taken as  $g_{\parallel}$ . Again the deviation of  $g_{\parallel}$  and  $g_{\perp}$  from the free-electron  $g_e$  value ( $g_e = 2.0023$ ), i.e.,  $\delta g_{\parallel} = g_{\parallel} - g_e$ ,  $\delta g_{\perp} = g_{\perp} - g_e$ , is actually used in the calculation.

Starting with the Hamiltonian which includes the spin-orbital interaction for a bound electron in a magnetic field, Watkins and Corbett<sup>4</sup> first gave the expression for the  $g_{\perp}$  shift, as  $\delta g_{\perp}$ . However, in the expression derived by them, the single electron is fully localized on one dangling bond nearest to the vacancy, and the symmetry reason requires that  $\delta g_{\parallel} = 0$ , where the parallel direction runs along the dangling bond. Considering that the bound electron is not fully localized on the dangling bond, Phillips<sup>16</sup> modified the expression for their  $g_{\perp}$  shift, and gave a more accurate formula

$$\delta g_{\perp} = \beta^2 \eta^2 \left[ \frac{1+\nu}{E_b} \lambda_b - \frac{1-\nu}{E_a} \lambda_a \right], \quad (22)$$

where  $E_b$  and  $E_a$  are the average excitation energies from the bound-electron state to the valence- and conduction-

band states, respectively.  $\lambda_b$  is the valence-band spin-orbital interaction parameter,  $\lambda_a$  is the conduction one, and the parameter  $\nu$  is a small correction due to the admixture of  $p$ -core states. Following Watkins and Corbett,<sup>4</sup> and Phillips,<sup>16</sup> we take  $\nu = 0.17$ ,  $\lambda_b = 0.029$  eV,  $\lambda_a = 0.015$  eV,  $E_b = 1.5$  eV, and  $E_a = 2.5$  eV; the  $\beta^2$  and  $\eta^2$  on the dangling bond will be obtained from Eqs. (18) and (19).

## V.. RESULTS AND DISCUSSION

Since the wave function  $\langle A' R m | \psi \rangle$  calculated from Eq. (10) is the function of the defect energy  $E$ , so the  $\eta_j^2, \alpha_j^2, \beta_j^2$  calculated from Eqs. (18) and (19), the  $a_j, b_j$  from (20),  $\theta$  from (21), and  $\delta g_{\perp}$  from (22) are the functions of the defect energy  $E$ . In order to obtain the optimum theoretical values describing the EPR and ENDOR of phosphorus-, arsenic-, and antimony-vacancy pairs, the energy  $E$  is scanned across the energy gap, from which the best results of our theory are selected. They are listed in Table II. There are no EPR or ENDOR experimental data for the bismuth-vacancy pair; we pick out of the maximum of  $\eta^2$  on the atom  $b$  (in Fig. 1) when the energy  $E$  of the defect scans the energy gap. In such a way, we calculate the  $a_j, b_j$ , and  $\eta_j^2, \alpha_j^2, \beta_j^2$  as the theoretical predictions for this defect.

Comparing the theoretical values with the experimental values in Table II, the following can be determined.

(i) For each of the centers, the theoretical values of the probability  $\eta_j^2$  and the percentage  $s$  and  $p$  character

TABLE II. Calculated hyperfine interaction constants  $a_j, b_j$ , direction  $\theta$ , the corresponding wave function  $\eta_j^2, \alpha_j^2, \beta_j^2$ , the energy level  $E$ , and  $g$  tensor shift  $\delta g_{\perp}$  of the group-V-impurity vacancy. The number in the round brackets is the experimental value from Refs. 4 and 5. Ellipses denote none of the corresponding values.

Defect center	Atom site	$a_j$ ( $10^{-4}$ cm $^{-1}$ )	$b_j$ ( $10^{-4}$ cm $^{-1}$ )	$\alpha_j^2$ (%)	$\beta_j^2$ (%)	$\eta_j^2$ (%)	$\delta g_{\perp}$ (%)	$\theta$ (deg)	$E$ (eV)
PV	Si(1)	137.9 (115.7)	12.80 (17.2)	21 (14)	79 (86)	47.8 (59)	6.7 (8.1)	35.5 (35.3)	0.67 (0.68)
	Si(2),Si(3)	13.14 (12.4)	0.86 ( . . . )	26 (30)	74 (70)	3.5 (3.0)			
	P	9.32 (9.32)	0.46 (0.63)	36 (29)	64 (71)	0.7 (1.0)		168.7 (163.5)	
AsV	Si(1)	137.60 (115.8)	12.66 (16.9)	21 (14)	79 (86)	47.5 (59)	6.7 (7.6)	35.5 (35.3)	0.67 (0.69)
	Si(2),Si(3)	12.28 ( . . . )	0.85 ( . . . )	26 ( . . . )	74 ( . . . )	3.4 ( . . . )			
	As	15.2 (14.4)	0.77 (0.8)	35 (32)	65 (68)	1.0 (1.0)		167.4 (144.7)	
SbV	Si(1)	136.80 (115.5)	12.33 (16.2)	21 (15)	79 (85)	46.4 (57)	6.5 (8.7)	34.8 (35.3)	0.69 (0.72)
	Si(2),Si(3)	5.9 (4.6)	0.38 ( . . . )	28 (30)	72 (70)	1.5 (1.0)			
	Sb	117.9 (122.7)	8.77 (5.1)	26 (39)	74 (61)	5.7 (4.0)		152.6 (133.2)	
BiV	Si(1)	133.5	11.38	22	78	43.4	6.1	34.7	0.73
	Si(2),Si(3)	6.8	0.48	25	75	1.8			(0.77)
	Bi	. . .	. . .	24	76	8.2		151.3	

$\alpha_j^2, \beta_j^2$ , localized on the respective Si(1) site remain unaltered, which is in agreement with experimental observation. In each case, there are the theoretical values, the probability  $\eta^2 \sim 50\%$  is localized on a single unpaired silicon atom, and the  $s$  character  $\alpha^2 \sim 20\%$ , and  $p$  character  $\beta^2 \sim 80\%$ . However, the theoretical value  $\eta^2$  is 83% of the experimental value. For a proper set of basis functions the value  $\eta_j^2$  should add up to 100%, which is satisfied by our basis function. Sievert *et al.*<sup>17</sup> always pointed out in their divacancy experiment that the value  $\sum_j \eta_j^2 = 119\%$  was determined by the ENDOR spectra. If the experimental value  $\sum_j \eta_j^2$  for the  $PV$ ,  $AsV$ ,  $SbV$ , and  $BiV$  were also such a case, then there would be  $(\sum_j \eta_j^2)_{\text{theor}} / (\sum_j \eta_j^2)_{\text{expt}} \approx 83\%$ . This is probably the main reason why the theoretical value  $\eta^2$  is smaller than the experimental value. In addition, the theoretical value  $\alpha^2$  ( $\beta^2$ ) is larger than (smaller than) the experimental value. The reason is that the relaxation of the silicon located on site (1) is neglected in our theory.

(ii) The theoretical value shows that the probability  $\eta^2$  on the impurity atom as it goes from phosphorus to antimony is seen to increase from  $\sim 0.7\%$  to  $1.0\%$ , and to  $5.7\%$ , and the amount of these values is near the experimental value. So the theory describes well the fact "seen" by the EPR and ENDOR<sup>4,5</sup> that the probability  $\eta^2$  on the impurity-atom site is increased with the atomic weight of the atom occupying that site. Inspection of Table II shows that the attractive potential introduced by the impurity atom is decreased with the atomic weight of the atom occupying that site. Thus we conclude that the probability  $\eta^2$  on the impurity atomic site is increased due to the decrease of the attractive short-range potential on this site, which is difficult to understand.

(iii) Another theoretical result consistent with the experiments is that accompanying the increase in the probability  $\eta^2$  on the impurity atom site is a corresponding decrease in the  $\eta^2$  on the sites of the two paired silicon atoms [Si(2) and Si(3)]. As an example, for  $PV$ , there is  $\sim 0.7\%$   $\eta^2$  on the impurity atom, while there is  $\sim 7.0\%$   $\eta^2$  on the Si(2) and Si(3) sites; for  $SbV$ , there is  $\sim 5.7\%$  of  $\eta^2$  on the impurity atom, and only  $\sim 1.5\%$  of  $\eta^2$  on the Si(2) and Si(3) sites.

(iv) The sum of the  $\eta^2$  on the four nearest neighbors surrounding the vacancy is  $\sim 55\%$  (in Table II), which also remains unaltered for each of the centers. Our calculation still shows that the sum  $\sum_j \eta_j^2$  on the atoms of the seven shells is  $\sim 87\%$ , which is similar to the case of a single vacancy in silicon.<sup>7</sup>

(v) The calculated  $a$  and  $b$  on the Si(1) site for each of the centers are nearly the same, which is in agreement with the observation by ENDOR. But the amount of these values deviates from the experimental values by  $\sim \pm 20\%$  due to neglecting the relaxation of the atom on the Si(1) site. The calculated  $\theta$  and  $\delta g_{\perp}$  on this silicon atom are also in agreement with the experiments. The calculated  $a$  or  $b$  on the remaining three atoms in Table II, agree well with the experiments.

(iv) The experimental values of  $a_j$  and  $b_j$  for the Si(2) and Si(3) sites of the  $PV$  and  $SbV$  are estimated by Watkins and Corbett,<sup>4</sup> and Elkin and Watkins,<sup>5</sup> from their EPR and ENDOR spectra, not directly measured. The

experimental values of  $\alpha^2$  and  $\beta^2$  were assumed by them in order to calculate  $\eta^2$  for these sites. The corresponding calculated values coincide with their values, so their estimated and assumed values are confirmed. There are no experiment values for the Si(2) and Si(3) of the  $AsV$ , but we believe these theoretical values to be reasonable.

(vii) For each of the centers, the energy levels determined by the theory with the data of the EPR and ENDOR spectra, are very nearly the energy levels from the existing experiments. The theory and experiments all indicate that the  $A'$  energy levels for these defects are insensitive to the change in the impurity potential, and near the energy of  $\sim 0.7$  eV. In previous work, we showed that energy level of an isolated single ideal vacancy ( $T_d$  symmetry) in silicon is equal to  $\sim 0.76$  eV. As in the analysis of Sankey and Dow,<sup>6</sup> by the defect pairs "molecule" model, the substitutional-impurity-vacancy pair senses the  $C_{3v}$  symmetry and produces one twofold-degenerate  $E$ -symmetry molecule level in the gap which should be essentially the same energy as the isolated vacancy  $T_2$  energy level. Hence the Jahn-Teller distortion is included, and the  $E$ -symmetry level is split into both state  $A'(C_{1h})$  and state  $A''(C_{1h})$ . The antibonding state  $A''$  may be driven upward in the conduction band or near the band edge; the bonding state  $A'$  remains in the gap and its energy is shifted down. Obviously, the magnitude of the distorted energy should be roughly equal to the energy difference between the single vacancy and the impurity vacancy, namely, the change in energy due to the Jahn-Teller distortion is 0.1 eV. This order of magnitude is contrary to the results of earlier calculations.<sup>5</sup>

(viii) The theoretical values of the wave function ( $\alpha^2$  and  $\beta^2, \eta^2$ ) and hyperfine interaction ( $a, b$ ) for  $BiV$  appear reasonable from the point of view of a similar configuration in the above three centers. This means that these theoretical values could serve as a useful guide for experiments.

## VI. CONCLUSION

From a consideration of the symmetry, the electronic state of the  $PV$ ,  $AsV$ ,  $SbV$ , and  $BiV$ , are entirely  $A'(C_{1h})$  symmetric. The wave function is obtained using the Green's-function method in the extended-potential approximation, and the combination of the tight-binding theory of band structures with the theory of defects of Hjalmarson *et al.* has been very successful in describing the similarity among the spectra of the group-V-impurity-vacancy pairs. Our theoretical results confirm the estimate and assumptions of Watkins *et al.* about the Si(2) and Si(3) for  $PV$  and  $SbV$  and eke out, empty of the atomic spectra of Si(2) and Si(3), sets for the  $AsV$ . We predict the hyperfine interaction for the  $BiV$ , and we have reason to believe that these theoretical values are more reasonable. It appears to us that there are few dissimilarities among these defects and their only difference is due to different magnitudes of the potential introduced by impurities, besides the relaxation of the unpaired silicon atom. Adopting the defect-pair "molecule" of Sankey and Dow,<sup>6</sup> the change in the energy level due to the Jahn-Teller distortion is estimated and the other of the magnitude  $\sim 0.1$  eV is given.

- <sup>1</sup>E. G. Sievert, *Phys. Status Solidi B* **120**, 11 (1983).
- <sup>2</sup>E. Soder and L. C. Templeton, *J. Appl. Phys.* **34**, 3295 (1963).
- <sup>3</sup>M. Hirata, M. Hirata, and H. Saito, *Jpn. J. Appl. Phys.* **5**, 252 (1966).
- <sup>4</sup>G. D. Watkins and J. W. Corbett, *Phys. Rev.* **134**, A1359 (1964).
- <sup>5</sup>E. L. Elkin and G. D. Watkins, *Phys. Rev.* **174**, 881 (1968).
- <sup>6</sup>O. F. Sankey and J. D. Dow, *Phys. Rev. B* **26**, 3243 (1982).
- <sup>7</sup>X.-Q. Fan, D.-X. Zhang, and S.-G. Shen, *Acta. Phys. Sin.* **37**, 177 (1988) (in Chinese).
- <sup>8</sup>X.-Q. Fan, S.-G. Shen, and D.-X. Zhang, *Acta. Phys. Sin.* **38**, 908 (1989) (in Chinese).
- <sup>9</sup>X.-Q. Fan, S.-G. Shen, and D.-X. Zhang, *Acta. Phys. Sin.* **38**, 914 (1989) (in Chinese).
- <sup>10</sup>S.-G. Shen, X.-Q. Fan, D.-X. Zhang, and S.-Y. Ren, *Acta. Phys. Sin.* (in Chinese) **39**, 970 (1990).
- <sup>11</sup>H. P. Hjalmarson, P. Vogl, D. J. Wolford, and J. D. Dow, *Phys. Rev. Lett.* **44**, 810 (1980); W. Y. Hsu, J. D. Dow, D. J. Wolford, and B. G. Streetman, *Phys. Rev. B* **16**, 1597 (1977).
- <sup>12</sup>Y.-Q. Jia and G.-G. Qin, *Phys. Rev. B* **37**, 2605 (1988).
- <sup>13</sup>P. Vogl, H. P. Hjalmarson, and J. D. Dow, *J. Phys. Chem. Solids* **44**, 365 (1981).
- <sup>14</sup>D. A. Papaconstantopoulos and E. N. Economou, *Phys. Rev. B* **22**, 2903 (1980).
- <sup>15</sup>D. J. Chadi and M. L. Cohen, *Phys. Rev. B* **8**, 5747 (1973).
- <sup>16</sup>J. C. Phillips, *Comm. Solid State Phys.* **3**, 67 (1970).
- <sup>17</sup>E. G. Sievert, S. H. Muller, and C. A. J. Ammerlaan, *Phys. Rev. B* **18**, 6834 (1978).